12th International Conference on Structural Analysis of Historical Constructions
SAHC 2020
P. Roca, L. Pelà and C. Molins (Eds.)

# SIMPLEX ALGORITHMS FOR 3D LIMIT ANALYSIS OF ROMAN GROIN VAULTS

**C. BAGGIO[1*], S. SANTINI[2]**

[1]Dipartimento di Architettura
Roma Tre University
Largo Marzi 10, 00153 Rome, Italy
e-mail: carlo.baggio@uniroma3.it (*corresponding author)

[2] Dipartimento di Architettura
Roma Tre University
Largo Marzi 10, 00153 Rome, Italy
email: silvia.santini@uniroma3.it

**Keywords:** Historical Structure, Masonry, 3D limit analysis

**Abstract** *In Roman Baths the Romans employed groin vaults of great dimensions, with maximum span more than 20 m; simple tools of structural analysis of ancient wide span vaulted halls are still lacking, due to geometrical and material complexity. In this paper we study the collapse behavior, under horizontal static action, of a corner cross vault of the Baths of Diocletian in Rome (Hall I). In the present modeling, masonry is discretized as a system of interacting rigid bodies in no-tension and frictional contact. The computational code consists in a linear programming approach which make use of a series of optimization packages via lower and upper bound techniques of limit analysis. In the paper, a solution strategy based on a modified simplex algorithm has been introduced in order to manage the large number of contacts given by a 3D block assembly. One more task of the proposed problem consists in a suitable description of the overall 3D geometry, here afforded with a specific pre-processing approach.*

## 1 INTRODUCTION

During the course of many centuries after the fall of the roman empire the buildings of the Baths underwent a gradual and progressive damage, the site became desolate, wasted and encumbered by ruins, as witnessed by a large number of drawings and engravings by sixteenth century landscapists and artists.

In Italy, the current building code (NTC 2018) requires historical analysis of existing masonry buildings as a pre-requisite for the design of structural conservation; this implies survey of resisting system, collecting data about transformation during life of building, often very long, reconstruction of special events, like seismic ones.

This task was managed by a historical reconstruction of the original vaulted system of the main body of the Baths, by research mainly devoted to collect historical images of ruined portion, trying to establish the sequence of collapses during XVI-XVII centuries (Nizzi &

Baggio 2014).

The structural system of the main body of the baths can be easily understood: larger central groin vaults are counteracted by secondary, peripheral barrel and groin vaults which conduct the thrust action to buttresses and foundations.

Nonetheless a number of questions arise: are the pillars of each vault able enough to resist to thrust or they need also aid from the adjacent walls? How can we measure the relative weakness of the partially ruined vaults?

Thus, in this paper, trying to give a quantitative answer, the authors adopt a numerical procedure based on 3D standard limit analysis according to the Italian Code for masonry structures, in particular for historic masonry and monuments. The limit analysis method for the seismic assessment of masonry structures is well known but application to real vaulted structures is far less common in literature. The proposed procedure is based on a mechanical model already discussed in previous work [Baggio & Trovalusci 2000, 2016]. The main improving, with respect to the previous analyses, concerns geometrical model, pre-processing and solution strategies.

**Figure 1**: Side photograph of Hall I

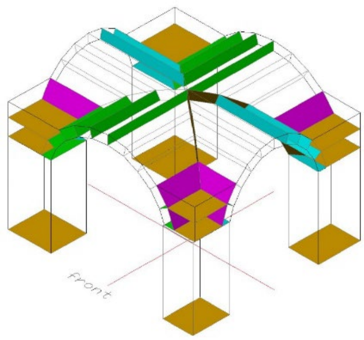


**Figure 2**: joints: pillar (yellow), abutment (magenta), voussoir (green and cyan), rib (brown)

## 2 PROPOSED APPROACH

The central body of the Baths is made of a series of seven aisles with semicircular barrel vaults intersecting three aisles; outer groin vaults of minor dimensions provide counteraction of thrust of central vaults. In this study the proposed procedure is applied to the corner groin vault called Hall I (see Figure 1).

The main difficulty in defining the geometrical model consists on a suitable description of the overall 3D assembly; setting up of a 3D mesh with non-trivial geometry becomes rapidly cumbersome and discouraging without the help of a tool to simplify the task. To this aim, the authors in the present work propose a procedure based on the following steps:

- drawing of the vault geometry directly by using AutoCAD;
- modeling of each body or hexahedron as solid element;
- modeling of each interface or joint as 'region', that is, an oriented plane surface. Figure 2 illustrates the pillar joints (yellow), the abutment joints (magenta), the

voussoir joints of the vaults (green and cyan) and the rib joints (brown); note that the positive orientation of the local z-axis is represented by color, whereas the rear blank face represents the negative orientation;

- exporting, from AutoCAD model, bodies and regions in a .SAT file which describes the topology of bodies by elementary sub-entities: faces, coedges, edges, vertices and points;
- producing data for the analytical model input, by means of a FORTRAN procedure developed by the authors able to interpret the SAT database. Data extracted by SAT file automatically generate coordinates of the 8 vertices of each hexahedron, mass and center of mass of each body, dimensions, center and orientation of interfaces, preventing data errors and facilitating plotting.

## 3 LIMIT ANALYSIS AND COLLAPSE MULTIPLIER

Roman masonry should be modeled properly as a continuum material with some resistance in tension; it could hardly be represented as assemblies of blocks with no tension and frictional interfaces. Nevertheless the proposed methodology succeeds in picking out the main characteristics of the behavior of a complex vaulted structure, as shown below.

Masonry assemblages are described as systems of n rigid prismatic blocks connected by no-tension and frictional interfaces through m plane contact surfaces. The blocks can translate and rotate: **u** (6n) is the vector of the generalized blocks displacement. Considering as strain measures of the assembly the relative displacements and the relative rotations between blocks, the kinematic compatibility equations are

$$\boldsymbol{C}\boldsymbol{u} = \boldsymbol{q} \tag{1}$$

where **q** (6*m*) is the vector of relative joint displacements and **C** is the kinematic matrix.

Vector **q** can be expressed as linear combination of p elementary modes of failure at each interface; typically p for quadrilateral contact surfaces is 14: 4 rotations about four edges, 8 slidings, 2 in-plane rotations

$$\boldsymbol{q} = \boldsymbol{M}\,\boldsymbol{\lambda} \tag{2}$$

where M (6m x pm) is a diagonal matrix containing geometrical coefficients and $\lambda$ (pm) is the vector of the failure modes. Contact surfaces of different shapes (octagonal for instance) can be also considered simply by suitably varying the matrix of the c-th contact, increasing the number of columns, thence increasing the number of unknowns.

Most of the interfaces have trapezoidal shape varying from one joint to the other, so each contact involves the writing of a specific matrix $\mathbf{M}_c$. Anyway in the most of cases, all the contacts have quadrilateral shape so the number of elementary failure modes p, remains unchanged, equal to 14 for each interface.

The actions on the blocks are permanent loads, represented by the vector of generalized 'dead' loads $\mathbf{f}_0$ (6n), and proportionally increasing loads, represented by the vector $\alpha\mathbf{f}_L$, where $\mathbf{f}_L$ (6n) is the generalized 'live' loads vector and $\alpha$ the unique (non-negative) parameter governing the load increasing. For the sake of clarity, the limit value of $\alpha$, $\alpha_c$, is named "collapse multiplier" or "load factor".

The balance equations for the assembly are

$$\boldsymbol{C}^{\mathrm{T}}\boldsymbol{Q} = \boldsymbol{f}_0+\alpha\boldsymbol{f}_{\mathrm{L}} \tag{3}$$

The blocks interact through forces and couples, ordered in the vector of the generalized stresses **Q** (6m). As the joints cannot carry tension and the tangential forces at the interfaces, as well as the in-plane couples (torques), are limited by the friction, bounds on the stress components must be imposed. These bounds define a piece-wise linear yield domain, represented by the inequalities

$$\boldsymbol{\phi} = \boldsymbol{N}^T\boldsymbol{Q} \leq \boldsymbol{0} \tag{4}$$

where $\mathbf{N}^{\mathrm{T}}$ (p$m$ x 6$m$) is the so-called gradient matrix.
To the 'activation' of a single face of the yield domain a relative displacement corresponds in such a way that

$$\boldsymbol{\phi}^T \boldsymbol{\lambda} = 0 \tag{5}$$

In the case of limit bending the vector **q** is normal to the active yield face, while in case of limit shear and limit torque it is not normal to the face (**M** ≠ **N**), so giving rise to a non-standard, non-linear, non convex, problem.

The evaluation of the collapse load and the collapse mechanism of Lagrangian systems of elements interacting through no-tension and frictional contact surfaces corresponds to the Limit Analysis of discretized rigid perfectly-plastic systems with non-associative flow rules. Due to the absence of stability criteria, the solution of the problem of searching the minimum load factor satisfying the Equations (1)-(5) has not unique solution.

In many cases the linearized solution is comparable with the non-linear one, both in terms of collapse mechanism and in terms of collapse multiplier $\alpha_c$.

From an operating point of view moreover, the introduction of spatial problems highly complicates the numerical task: in systems of blocks connected together in three-dimensional arrangements, the number of contacts per block highly increases, producing a significant overdeterminacy of the kinematic problem. Use of linearized analysis simplifies the numerical task and leads almost always to acceptable results. In this study only LP approach has been used.

A Gauss-Jordan elimination allow to split matrix **C** in two parts: $\mathbf{C}^{\mathrm{I}}$, a square matrix of maximum rank and $\mathbf{C}^{\mathrm{II}}$, together with a correspondent separation of **q** in $\mathbf{q}^{\mathrm{I}}$, $\mathbf{q}^{\mathrm{II}}$ and **Q** in $\mathbf{Q}^{\mathrm{I}}$, $\mathbf{Q}^{\mathrm{II}}$.
Defining two matrices $\mathbf{A}_0$, **A** as

$$\boldsymbol{A}_0 = [(\boldsymbol{C}^I)^{-1} \;\; \boldsymbol{0}] \qquad\qquad \boldsymbol{A} = [\,-\boldsymbol{C}^{II}(\mathbf{C}^I)^{-1} \quad \boldsymbol{I}] \tag{6}$$

from standard algebraic manipulation it follows

$$\boldsymbol{u} = \boldsymbol{A}_0\, \boldsymbol{q} \tag{7}$$

with constraint of kinematic compatibility

$$\boldsymbol{A}\, \boldsymbol{q} = \boldsymbol{0} \tag{8}$$

and

$$\boldsymbol{Q} = \boldsymbol{A}_0^T(\boldsymbol{f}_0+\alpha\boldsymbol{f}_L)+\boldsymbol{A}^T\boldsymbol{Q}^{II}. \tag{9}$$

A standard limit analysis can be performed by means of upper bound or lower bound approach.
In the first case, upper bound approach, the linear problem (LP) is written as

$$\begin{aligned}
&\textit{Determine min } \{\alpha = -\boldsymbol{\lambda}^T(\mathbf{A}_0\mathbf{M})^T\mathbf{f}_0\} \text{ subjected to:} \\
&\mathbf{AM\lambda = 0} \\
&\boldsymbol{\lambda}^T(\mathbf{A}_0\mathbf{M})^T\mathbf{f}_L = 1
\end{aligned} \tag{10}$$

with the unknowns $\boldsymbol{\lambda} \geq \mathbf{0}$, $\alpha \geq 0$. $\mathbf{Q}^{II}$ are obtained as dual unknowns from the optimization routine.
In the second case, lower bound approach, the LP is

$$\begin{aligned}
&\textit{Determine max } \{\alpha\} \text{ subjected to:} \\
&(\mathbf{AN})^T\mathbf{Q}^{II} + \alpha(\mathbf{A}_0\mathbf{N})^T\mathbf{f}_L + (\mathbf{A}_0\mathbf{N})^T\mathbf{f}_0 \leq \mathbf{0}
\end{aligned} \tag{11}$$

with the unknowns $\mathbf{Q}^{II}$, $\alpha$.
In this second problem the kinematic unknowns $\boldsymbol{\lambda}$ are obtained by the optimization routine as dual results. Note that for standard limit analysis $\mathbf{M} = \mathbf{N}$.

## 4 NUMERICAL SIMULATION

### 4.1 Modeling of masonry vaults by limit analysis

This paper examines only an outer groin vault (covering a corner hall) of minor dimensions, because the larger central vaults are counteracted by a series of barrel vaults on the south-west front and by large pillars or buttresses on the opposite front, towards the ‘natatio’ (swimming pool).

As part of a research work devoted to assess the safety of the structures of the Baths with particular reference to seismic actions, the live external load, $\mathbf{f}_L$, is represented by horizontal body forces which statically simulate the seismic action.

Hall I is rectangular in plan, so the orthogonal gores show different vault spans: 13.7 m the front span and 10.7 m the orthogonal one, with thickness of about 110 cm. The impost of the vault is 9.7 m above ground level. Dimensions of pillars in plan vary from 3.65 to 5.15 m.

The material of pillars and vaults is ‘opus caementicium’ that is roman concrete made by an aggregate of tufa rubble stone and a hydraulic mortar of lime and pozzolana.

As said above this material should be modeled properly as a continuum material with some resistance in tension; for future development a moderate tension resistance will be introduced in the 3D model, as already made in 2D models.

However the continuum behavior of this kind of masonry strongly depends on parameters not always easily determinable, so a discrete approach is sometimes preferable.

The model involves 52 bodies or blocks of hexahedral shape and 92 quadrilateral contact faces. This means that in case of upper bound approach the problem has 1288 kinematical unknowns $\boldsymbol{\lambda}$ and 241 constraint equations, otherwise in case of lower bound approach the problem has 240 static unknowns $\mathbf{Q}^{II}$, plus $\alpha$, i.e. 241 unknowns and 1288 constraints equations. Exchange between number of constraints and number of unknowns comes from the duality of the two approaches.

Authors know by experience that the LP problem, even if it is linear or linearized, often encounters numerical difficulties in finding correct results; for this reason the number of units chosen to constitute the structure is limited, anyway the very restriction concerns the number of units used to model the gores, whereas the limited number of the pillar blocks doesn't affect the result. Note that abutment units have been inserted in the model since these masses are able to counteract the thrust of the vaults and to stabilize the pillars with their load. At last, the model doesn't take into account masonry walls of minor thickness resting between the bearing pillars.

### 4.2 Solution strategy

As described above the model data need algebraic manipulation before passing them to an optimization routine; manipulation consists in creation of vectors and matrices, inversion, transposition, binding of matrices and multiplication of matrices by vectors. To speed up the procedure all this operations are automatically performed in sequence by a series of FORTRAN routines. All the process requests a handful of seconds also with large dimension problems.

Above recalled numerical difficulties in optimization process recommend to proceed step-by-step solving, in advance, sub structures, namely parts of the entire vault.

This strategy, moreover, permits to detect and correct errors in the numerical model.

The real Achilles' heel of the whole procedure are the minimization routines: more or less all of the attempted approaches showed to be inefficient in solving problems with a moderately large number of unknowns and constraints.

We tested the 'revised simplex method' in IMSL MATH Library running in FORTRAN and a number of linear optimization routines in the MATLAB environment: these are 'simplex', 'dual simplex', 'interior point legacy' and 'active set' methods.

All of the tested methods failed to reach a solution for the upper bound approach when calculating the optimal point for the larger model, the complete one.

It appeared that the numerical problem was beyond the capacity of all the tested optimization programs. This fact is worthy of discussion.

The simplex method, pretty well known and easy to understand from a theoretical point of view, fails to find a starting point, named 'feasible point', to begin search of the optimal solution and give a warning: 'infeasible problem'; moreover warns about the 'strictness of equality constraints'.

Really, the upper bound approach (see eq. 10) introduces in the algorithm equality constraints, which complicates the finding of a starting 'feasible point'.

So we reverted to use the lower bound technique (see eq. 11) where there are a greater number of constraint equations but these are inequality constraints, so less stringent than in the first case. Finally, an explanation of the difficulties encountered by numerical problem may depend also on the real complexity of the problem; as will be seen below the collapse mechanism activates many faces of the yield domain at the same time, due to the static indeterminacy of the structure, because of a largely greater number of joints with respect to the number of bodies (see for instance Figure 4).

### 4.3 Results of analyses

The first attempt to carry out an analysis on a substructure is plotted in figure 3: two opposite gores interacting only between joints at the apex of the vault. Direction of horizontal mass action is also depicted in the figure. Due to reduction of number of unknowns and restraints in the model, this numerical problem results easy to be solved by all the optimization routines described above. The kinematic mechanism involves the overturning of two of the four pillars and an arch-like behavior of the two opposite gores. This is, in fact, the standard in-plane behavior of an arch without a steel tie rod, which would oblige the pillars to overturn jointly (Baggio 2009). It can be seen, also, the formation of three cylindrical hinges in the arch at the intrados – extrados – intrados, alternatively, as in an arch, and the fourth hinge at the foot of the right pillar.

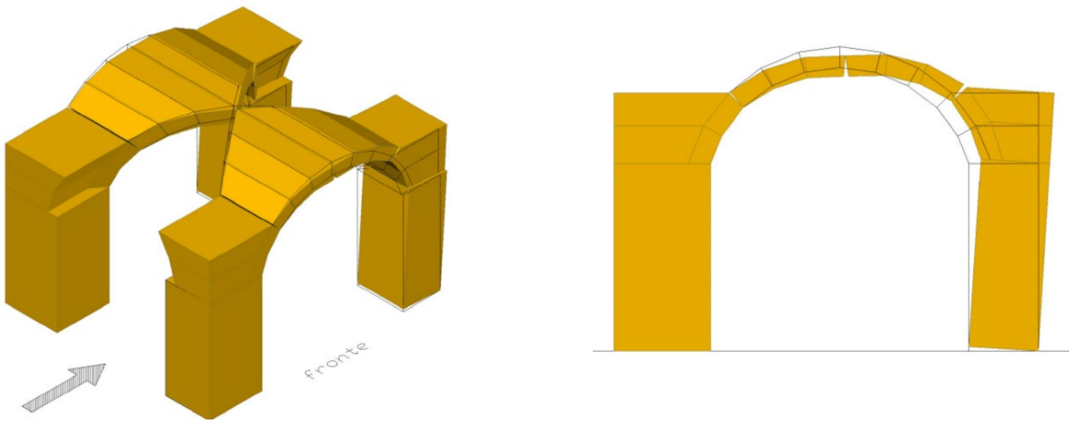


**Figure 3**: Two opposite gores, axonometric and front view of the collapse mechanism, $\alpha_c = 0.116$

The value of the collapse multiplier $\alpha_c = 0.116$ shows that this structure would be relatively weak, unable to withstand an earthquake as expected in Rome, according to the Italian Building Code.

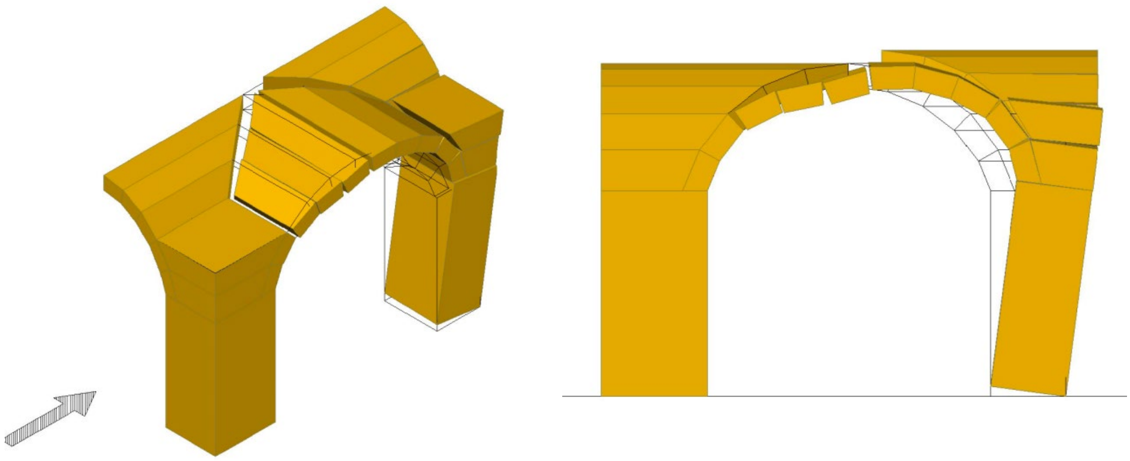

**Figure 4**: Half symmetric vault: axonometric and front view of the collapse mechanism, $\alpha_c = 0.269$

The second test has been carried out on a symmetric half vault (figure 4). The structure is restrained along the middle axis by external interfaces which act as simple supports with a very low friction coefficient (f = 0.1); again numerical difficulties prevent the reaching of a correct solution when putting to zero the friction in that joints. This fact probably interferes with the collapse mechanism, forcing again an arch-like behavior, but producing a far higher value of the collapse multiplier ($\alpha_c = 0.269$).

In figure 4 can also be observed a number of gaps in some joints; use of linear optimization, as would be correct in presence of associate flow rule implies the introduction of dilatancy in the interfaces. When sliding occurs it give rise to a correspondent normal component of displacement producing the observed gaps. In other words friction is replaced by dilatancy.

The analysis of the complete model in Figure 5 finds out a collapse multiplier $\alpha_c$ comparable with that found for the half model, whereas the mechanism involves the overturning of the four pillars, showing a tridimensional behavior far from in-plane behavior of arches.

A conclusion can also be drawn regarding the safety assessment of the Hall I in the Baths; according to Italian Seismic Code, spectral acceleration required in comparison with the calculated collapse multiplier $\alpha_c$ should vary from 0.12 to 0.20, depending on the accepted return period of the expected earthquake. The complete cross vault analyzed ($\alpha_c = 0.284$) is able to withstand future quakes without need to insert steel tie rods or other strengthening apparatus.

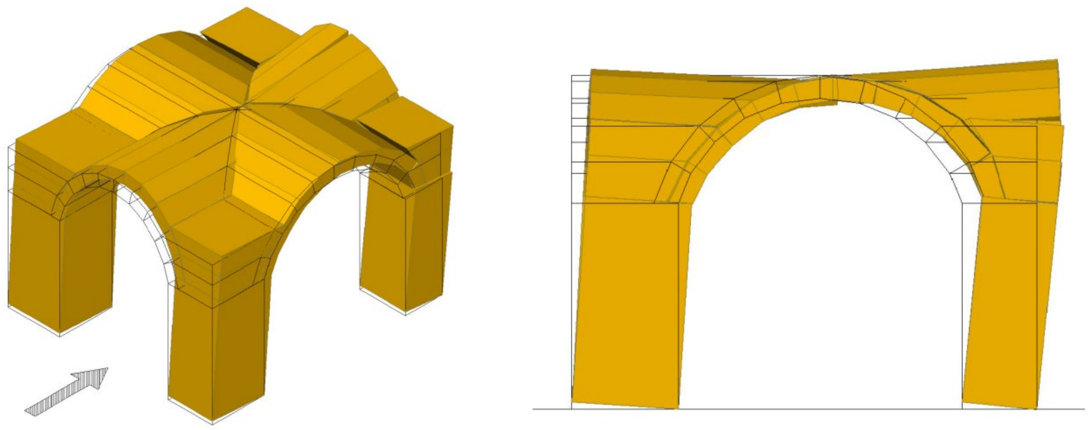

**Figure 5**: Complete model, axonometric and front view of the collapse mechanism, $\alpha_c = 0.284$

## 5 A MODIFIED SIMPLEX ALGORITHM

With the attempt to overcome the numerical difficulties due to a large number of blocks and joints, it would be useful to have a proper optimization procedure.

In what follows, in order to specifically deal with the matters concerned, the adopted procedure that makes use of a modified simplex method will be described step by step.

An optimization tableau via the simplex method is usually represented as

$$\begin{vmatrix} 1 & -c^T & 0 \\ 0 & D & b \end{vmatrix} \tag{12}$$

in which the first row defines the objective function and the remaining rows define the constraints. If D can be rearranged to contain an identity matrix I, of maximum range nr (where nr is the number of rows), a tableau in canonical form becomes

$$\begin{vmatrix} 1 & 0 & -\underline{c}^T & z_b \\ 0 & I & E & b \end{vmatrix} \tag{13}$$

The variables corresponding to the columns of **I** are the “basic variables”, all other unknowns are the “non-basic variables”. The values of the basic variables are easily obtained by setting the non-basic variables equal to zero, in this case the basic variables are equal to the right-hand side **b**. The resulting objective function, even if not optimal, identifies a feasible point anyway.

Unfortunately, this procedure runs only for non-negative values of the right-hand side **b**.

A linear problem not given in canonical form could be managed by introducing *nr* artificial variables, s, named ‘slack variables’. A new objective function, $z_0$, is introduced as first row of the tableau as the sum of the slack variables.

$$\begin{vmatrix} 1 & 0 & 0 & -s^T & 0 \\ 0 & 1 & -c^T & 0 & 0 \\ 0 & 0 & D & I & b \end{vmatrix} \tag{14}$$

By minimizing the new artificial objective function $z_0$, again with the simplex method, the algorithm ends when $z_0=0$; this means that all the artificial variables assume zero value. As a consequence, the artificial objective function and the slack variables can be eliminated giving rise to a canonical tableau equivalent to the original problem.

In the present formulation, the constraint equations (eq. 10) have the right-hand side **b** which is zero, except for the last one term. This suggested a new approach aimed to obtain a feasible point. The procedure consists in a Gauss elimination on *nr*-1 columns and rows obtaining an identity matrix with range *nr*-1 and non negative b terms, that is a quasi-canonical tableau.

$$\begin{vmatrix} I & E & 0 \\ 0 & e_{nr}^T & 1 \end{vmatrix} \tag{15}$$

Again it is mandatory to introduce an artificial objective function, $z_0$, but the proposed procedure allows to introduce a single slack variable instead of *nr* ones. So the minimization of $z_0$ is much more manageable and numerically stable.

The linear problem described can be represented in *tableau form* as follows (Table I); the first two rows and columns correspond respectively to the artificial objective function and to the true objective function z. The crosshatch identifies matrix **I**, derived from the Gauss elimination.

**Table I** – Tableau form of the linear problem

| | $z_0$ | z | $x_1$ | $x_2$ | $x_3$ | $x_4$ | $x_5$ | $x_{nc}$ | s | RHS |
|---|---|---|---|---|---|---|---|---|---|---|
| row -1 | 1 | 0 | 0 | 0 | 0 | 0 | 0 | 0 | -1 | 0 |
| row 0 | 0 | 1 | 0 | 0 | 0 | e | e | e | 0 | 0 |
| row 1 | 0 | 0 | 1 | 0 | 0 | e | e | e | 0 | 0 |
| row 2 | 0 | 0 | 0 | 1 | 0 | e | e | e | 0 | 0 |
| row 3 | 0 | 0 | 0 | 0 | 1 | e | e | e | 0 | 0 |
| row nr | 0 | 0 | 0 | 0 | 0 | $e_{nr}$ | $e_{nr}$ | $e_{nr}$ | 1 | 1 |

A row addition of the last row to the first one, called *pricing out,* gives the second tableau (Table II), where the row -1 and the row nr became equal, except for the s column.

**Table II** – Pricing out

| | $z_0$ | z | $x_1$ | $x_2$ | $x_3$ | $x_4$ | $x_5$ | $x_{nc}$ | s | RHS |
|---|---|---|---|---|---|---|---|---|---|---|
| row -1 | 1 | 0 | 0 | 0 | 0 | $e_{nr}$ | $e_{nr}$ | $e_{nr}$ | 0 | 1 |
| row 0 | 0 | 1 | 0 | 0 | 0 | e | e | e | 0 | 0 |
| row 1 | 0 | 0 | 1 | 0 | 0 | e | e | e | 0 | 0 |
| row 2 | 0 | 0 | 0 | 1 | 0 | e | e | e | 0 | 0 |
| row 3 | 0 | 0 | 0 | 0 | 1 | e | e | e | 0 | 0 |
| row nr | 0 | 0 | 0 | 0 | 0 | $e_{nr}$ | $e_{nr}$ | $e_{nr}$ | 1 | 1 |

At this point the phase I begins, aiming to obtaining the minimum value of the $z_0$ function, indeed equal to 0. The phase I starts by choosing an entering variable, that's to say a new basic column (Table III).

**Table III** - Choosing an entering variable

| | $z_0$ | z | $x_1$ | $x_2$ | $x_3$ | $x_4$ | $x_5$ | $x_{nc}$ | s | | RHS |
|---|---|---|---|---|---|---|---|---|---|---|---|
| row -1 | 1 | 0 | 0 | 0 | 0 | $e_{nr}$ | $e_{nr}$ | $e_{nr}$ | 0 | | 1 |
| row 0 | 0 | 1 | 0 | 0 | 0 | e | e | e | 0 | | 0 |
| row 1 | 0 | 0 | 1 | 0 | 0 | e | e | e | 0 | | 0 |
| row 2 | 0 | 0 | 0 | 1 | 0 | e | e | e | 0 | | 0 |
| row 3 | 0 | 0 | 0 | 0 | 1 | e | e | e | 0 | | 0 |
| row nr | 0 | 0 | 0 | 0 | 0 | $e_{nr}$ | $e_{nr}$ | $e_{nr}$ | 1 | | 1 |

Phase I makes use of the simplex method; the task remains hard owing to the particular structure of the right hand side terms, which, at the beginning represent a degenerate vector (all the terms except one are 0) able to cause stalling or cycling. Numerical methods perform badly often, due to the fact that the matrix includes at the same time numbers too large or too small in magnitude.

The presented method try to avoid initial numerical difficulties performing a Gauss elimination with full pivoting so that the E matrix contains number not too different in magnitude.

The proposed procedure nonetheless succeeds to reach almost always a correct result. In this case, when $z_0 = 0$, the artificial variable, s, can be eliminated, together with the column -1 and the row -1, producing a canonical tableau equivalent to the original problem (Table IV).

**Table IV –** Canonical tableau

| | | z | $x_1$ | $x_2$ | $x_3$ | $x_4$ | $x_5$ | $x_{nc}$ | RHS |
|---|---|---|---|---|---|---|---|---|---|
| objective f. | row 0 | 1 | 0 | 0 | 0 | e | 0 | e | $b_z$ |
| constr. eq. | row 1 | 0 | 1 | 0 | 0 | e | 0 | e | b |
| " | row 2 | 0 | 0 | 1 | 0 | e | 0 | e | b |
| " | row 3 | 0 | 0 | 0 | 1 | e | 0 | e | b |
| " | row nr | 0 | 0 | 0 | 0 | e | 1 | e | b |

The canonical tableau in Table IV represents a *feasible solution*; this one could be passed to a standard simplex routine for Phase II, avoiding the problems described in 3.2. The 3D arch in Figure 6, performing phase I, converges after 2 iterations only. 50 iterations are necessary to complete the phase II, reaching the optimum value of the collapse multiplier $\alpha_c$.

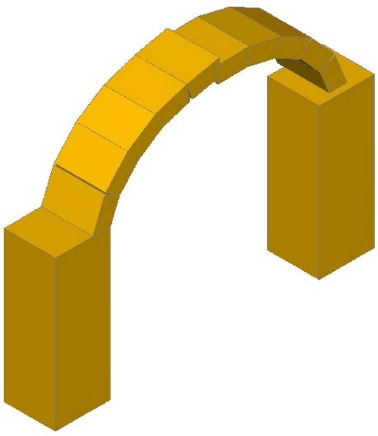

**Figure 6:** 3D arch model – $\alpha_c = 0.187$

## 6 CONCLUSIONS

The proposed methodology, even though discrete, succeeds in picking out the main characteristics of the behavior of complex vaulted structure, evaluating and quantifying the relative weakness of ruined cross vaults. It also gives an answer to question posed in the introduction: the pillars of each vault are able to withstand to thrust without contribution from adjacent walls.

In the paper, an original solution strategy aimed to overpass the common difficulties given by the application of linear optimization algorithms has been implemented with satisfactory results in terms of both collapse mechanisms and collapse multipliers. The strategy is based on a modified simplex algorithm which allows to obtain a quasi-canonical tableau preliminary to the running of the optimization procedure.

A specific preprocessor able to manage the complexity of the overall 3D geometry, has also been developed.

For future work a moderate, or random, tension resistance will be introduced in the model, to better represent roman concrete. Effects of foundation settlements could also be analyzed, simply by varying some constant terms in the eq. 10 and the live load.

**Acknowledgements.** We wish to express our special thanks to Dr. Rosanna Friggeri past director of the National Roman Museum – Baths of Diocletian, and to Arch. Marina Magnani Cianetti past supervisor of the restoration of the Ludovisi's cloister, recently open to museum visitors.

## REFERENCES

[1] Baggio, C. & Trovalusci, P. Collapse behaviour of three-dimensional brick-block systems using non-linear programming. *Structural Engineering and Mechanics* (2000), **10**(2): 181-195.

[2] Murty, Katta G. *Linear programming*, John Wiley & Sons (2000).

[3] Casapulla, C. & D'Ayala, D. Lower-bound approach to the limit analysis of 3D vaulted block masonry structures. In: TG. Hughes & GN. Pande (Eds): *Computer Methods in Structural Masonry*, Vol. *5, Swansea,* Computers & Geotechnics Ltd (2001), pp. 177-183.

[4] Ferris, M. & Tin-Loi, F. Limit analysis of frictional block assemblies as a mathematical program with complementarity constraints. *Int. J. Mech. Sci.* (2001), 43: 209-224.

[5] Baggio, C. Il restauro antisismico dei centri storici e la regola d'arte. *Ricerche di Storia dell'Arte* (2009), 99, 2: 19-29.

[6] Jackson, M. D., Logan, J. M., Marra, F., Scheetz, B. E., Deocampo, D. M., Cawood, C. G. Composizione e caratteristiche meccaniche dei calcestruzzi della grande aula, L. Ungaro, M. P. Del Moro, M. Vitti (Eds), *I mercati di Traiano restituiti – studi e restauri 2005-2007*, Roma, Palombi (2010), pp. 145-153.

[7] Nizzi, I. & Baggio, C. Vulnerabilità sismica delle grandi aule delle terme di Diocleziano. In: A. Centroni & M.G. Filetici (Eds): *Attualità delle aree archeologiche*; Atti del VII Convegno ARCo, Roma, 2014.

[8] Block, P., Lachauer, L. Three-dimensional (3D) equilibrium analysis of gothic masonry vaults. *Int. J. Architectural Heritage (2014)*, 8: 312-335.

[9] Baggio, C. & Trovalusci, P. 3D Limit analysis of Roman groin vaults, IBMAC 2016, Proc. 16th Int. Brick block Masonry Conf., Padua, Italy, CRC Balkema.